





Article

[¹⁸F]FDG PET/CT in Short-Term Complications of COVID-19: Metabolic Markers of Persistent Inflammation and Impaired Respiratory Function

Eva María Triviño-Ibáñez ^{1,2,†}, Beatriz María Jiménez-Rodríguez ^{2,3,4,†} , Teodoro Rudolphi-Solero ^{1,2,*} , Encarnación Yolanda García-Rivero ^{1,2}, Antonio Rodríguez-Fernández ^{1,2} , José Manuel Llamas-Elvira ^{1,2} , Manuel Gómez-Río ^{1,2,‡} and Concepción Morales-García ^{2,4,‡}

- ¹ Department of Nuclear Medicine, Virgen de las Nieves University Hospital, 18014 Granada, Spain; eva_gor@hotmail.com (E.M.T.-I.); encarnacion.garcia.rivero.sspa@juntadeandalucia.es (E.Y.G.-R.); antonio.rodriguez.fernandez.sspa@juntadeandalucia.es (A.R.-F.); josem.llamas.sspa@juntadeandalucia.es (J.M.L.-E.); manuel.gomez.rio.sspa@juntadeandalucia.es (M.G.-R.)
- ² Biosanitary Research Institute of Granada-IBS, 18012 Granada, Spain; beajirod@gmail.com (B.M.J.-R.); concepcion.morales.sspa@juntadeandalucia.es (C.M.-G.)
- ³ PhD P in Clinical Medicine and Public Health, Department of Microbiology, School of Medicine, University of Granada, 18011 Granada, Spain
- ⁴ Department of Pneumology, Virgen de las Nieves University Hospital, 18014 Granada, Spain
- * Correspondence: teorudsol@gmail.com
- † These authors contributed equally to this work.
- ‡ These authors contributed equally to this work.



Citation: Triviño-Ibáñez, E.M.; Jiménez-Rodríguez, B.M.; Rudolphi-Solero, T.; García-Rivero, E.Y.; Rodríguez-Fernández, A.; Llamas-Elvira, J.M.; Gómez-Río, M.; Morales-García, C. [¹⁸F]FDG PET/CT in Short-Term Complications of COVID-19: Metabolic Markers of Persistent Inflammation and Impaired Respiratory Function. *Diagnostics* **2022**, *12*, 835. <https://doi.org/10.3390/diagnostics12040835>

Academic Editor: Fabiano Di Marco

Received: 22 February 2022

Accepted: 24 March 2022

Published: 29 March 2022

Publisher's Note: MDPI stays neutral with regard to jurisdictional claims in published maps and institutional affiliations.



Copyright: © 2022 by the authors. Licensee MDPI, Basel, Switzerland. This article is an open access article distributed under the terms and conditions of the Creative Commons Attribution (CC BY) license (<https://creativecommons.org/licenses/by/4.0/>).

Abstract: SARS-CoV-2 virus infects organs other than the lung, such as mediastinal lymph nodes, spleen, and liver, but, to date, metabolic imaging studies obtained in short-term follow-ups of patients hospitalized with severe COVID-19 infection are rare. Our objective was to evaluate the usefulness of [¹⁸F]FDG-PET/CT in the short-term follow-up of patients admitted for COVID-19 pneumonia and to explore the association of the findings with clinical prognostic markers. The prospective study included 20 patients with COVID-19 pneumonia (November 2020–March 2021). Clinical and laboratory test findings were gathered at admission, 48–72 h post-admission, and 2–3 months post-discharge, when [¹⁸F]FDG-PET/CT and respiratory function tests were performed. Lung volumes, spirometry, lung diffusion capacity for carbon monoxide (DLCO), and respiratory muscle strength were measured. Volumetric [¹⁸F]FDG-PET/CT results were correlated with laboratory and respiratory parameters. Eleven [¹⁸F]FDG-PET/CT (55%) were positive, with hypermetabolic mediastinal lymphadenopathy in 90.9%. Mediastinal lesion's SUVpeak was correlated with white cells' count. Eleven (55%) patients had impaired respiratory function, including reduced DLCO (35%). SUVpeak was correlated with %predicted-DLCO. TLG was negatively correlated with %predicted-DLCO and TLC. In the short-term follow-up of patients hospitalized for COVID-19 pneumonia, [¹⁸F]FDG-PET/CT findings revealed significant detectable inflammation in lungs and mediastinal lymph nodes that correlated with pulmonary function impairment in more than half of the patients.

Keywords: COVID-19; [¹⁸F]FDG-PET/CT; respiratory function test; inflammatory; complications; SARS-CoV-2

1. Introduction

There is growing interest in the diagnosis, prognosis, and optimal clinical management of the sequelae of acute COVID-19 infection.

In the acute phase of infection, the epidemiology, clinical characteristics, results of standard clinical laboratory tests, lung CT appearance, treatment strategies, and outcomes in patients with COVID-19 have been reported in previous studies [1]. Imaging techniques, especially high-resolution computed tomography (HRCT), have demonstrated a relevant

diagnostic role [2], and multiple studies have been published on radiological findings in patients with COVID-19 pneumonia, especially during the acute phase and, more recently, over the short and medium terms [2,3].

The SARS-CoV-2 virus has been shown to infect organs other than the lung, such as the mediastinal lymph nodes, spleen, and liver, quantitative case studies in patients with COVID-19 are rare [3,4]. Such information can be obtained through the use of [¹⁸F]-2-Fluoro-2-Deoxy-Glucose ([¹⁸F]FDG) positron emission tomography/computed tomography (PET/CT), which is commonly used to assess inflammatory and infectious lung diseases [5].

The complementary functional information provided by [¹⁸F]FDG-PET/CT, which has been shown to be useful for diagnosing inflammatory and infectious lung diseases, estimating their severity, monitoring their evolution, and evaluating therapeutic response [4,5], can help elucidate the pathophysiological mechanisms of COVID-19. The value of [¹⁸F]FDG-PET/CT has been reported in patients with respiratory infections caused by other coronaviruses, such as MERS-CoV and SARS-CoV [6,7], as well as in patients with acute COVID-19 infection [4,8].

The [¹⁸F]FDG-PET/CT studies of asymptomatic cancer patients described the incidental detection of interstitial pneumonia compatible with possible acute SARS-CoV-2 infection [7], and researchers have begun to examine the potential role of [¹⁸F]FDG-PET/CT in its diagnosis and treatment [8]. As well as visual interpretation by an experienced specialist, [¹⁸F]FDG-PET/CT also offers a semiquantitative approach to glyceic metabolism and, therefore, the intensity of inflammatory activity. Besides the standardized uptake value (SUV), recent studies in oncology have yielded additional parameters such as the metabolic tumor volume (MTV) and total lesion glycolysis (TLG) [9], which could be used to estimate inflammatory activity in lungs or extrapulmonary organs, especially lymph nodes. Studies of noncritical hospitalized patients have highlighted the possible relevance of lymph node hypermetabolism, quantified by the maximum SUV (SUV_{max}) in PET images, proposing that the highest SUV_{max} values for lesions and lymph nodes may indicate an increased severity of the infection and may predict a poor prognosis [3,4].

With this background, we hypothesized that [¹⁸F]FDG-PET/CT could be useful to characterize pulmonary sequelae of COVID-19 infection. The objective of this study was to evaluate the usefulness of [¹⁸F]FDG-PET/CT in the short-term follow-up of patients admitted for COVID-19 pneumonia and to explore the association of findings with clinical prognostic markers

2. Materials and Methods

2.1. Patients

This prospective, longitudinal, observational study enrolled consecutive COVID-19 patients at their follow-up visit 1–2 months after discharge from a third-level hospital between 27 November 2020 to 1 March 2021.

Study inclusion criteria were confirmation of COVID-19 in accordance with WHO guidelines [10] by a positive RT-PCR result for nasopharyngeal swabs, hospital admission between November 2020 to March 2021 (dates of “third wave” in Spain), and findings of ground-glass opacity or consolidation on chest HRCT scan or X-ray at admission. Exclusion criteria were age under 18 years, absence of microbiological confirmation of COVID-19 infection, history or presence of pulmonary fibrosis, active or uncontrolled COVID-19 infection at the time of the [¹⁸F]FDG-PET/CT study, history or suspicion of oncological disease, pregnancy, and inability to sign informed consent.

The study was approved by the local Research Ethics Committee, and written, informed consent was obtained from all participants. Personal protective equipment was available for all staff, and COVID-19 infection prevention guidelines were always rigorously followed [11].

2.2. Clinical Information and Laboratory Test Results

For all patients, data were gathered from electronic medical records, including the results of clinical and laboratory tests at admission, at 48–72 h post-admission, and at the follow-up PET/CT examination. Analytical data included complete blood count, standard blood biochemistry, acute phase reactants, coagulation status [12], and neutrophil/lymphocyte ratios (NLRs). All patients underwent RT-PCR for nucleic acid testing of SARS-CoV-2.

2.3. Respiratory Function Tests

Respiratory function tests were performed at 2–3 months after hospital discharge. Spirometry results (in mL and % predicted) were obtained for forced vital capacity (FVC), forced expiratory volume in 1 s (FEV1), and FEV1/FVC ratio. Body plethysmography was used to measure the residual volume (RV, in mL and % predicted), and total lung capacity (TLC, in mL and % predicted). The diffusing capacity of the lungs for carbon monoxide (DLCO) and the CO transfer coefficient (KCO) were expressed in absolute numbers and as % predicted. The results of the 6-min walk test (TM6M) were expressed as distance (in m) and % oxygen saturation at start and finish. Specifically trained personnel carried out functional tests using MasterScreen Body equipment (Jaeger, Hoechberg, Germany), considering reference values for the Mediterranean population and acceptability criteria established by European and Spanish regulations [13,14].

2.4. PET/CT Data Acquisition

After two consecutive negative RT-PCR test results for SARS-CoV-2 nucleic acid, confirming that patients were no longer infected, patients underwent [¹⁸F]FDG-PET/CT imaging (Siemens Biograph Vision 600 PET/CT, Siemens Healthcare, Erlangen, Germany), always performed within 2–3 months after discharge from hospital. The test protocol was based on international recommendations [15]. Patients were administered intravenously with the radiopharmaceutical (3.7–4.81 MBq/kg) at rest after fasting for at least 6 h with adequate hydration as long as their capillary blood glucose level was below 6.8 mmol/L. Image acquisition (whole body in 3D) started at 50–60 min post-injection with the acquisition of a topogram (50 mA, 120 kV), followed by helical CT without contrast (170 mA, 120 kV) and the acquisition of PET images with coverage from skull base to mid-thigh.

2.5. PET/CT Image Interpretation

The [¹⁸F]FDG-PET/CT and chest CT images were independently analyzed by two nuclear medicine physicians (E.M.T.I. and M.G.M.) with a great deal of experience in the interpretation of cardiothoracic images, using syngo.via version VB40B software (Siemens Healthcare, Erlangen, Germany). They were blinded to the biological and clinical data of patients. Discrepancies in interpretations were resolved by consensus with a third expert nuclear medicine physician (A.R.F.).

The [¹⁸F]PET/CT data were transferred to a computer workstation (syngo.via) for the co-registration of PET and CT images. Regions of interest (ROIs) were drawn on CT images of lungs around areas with evident loss of aeration and adjacent areas of normal appearance. ROIs were also drawn on CT images of mediastinal lymph nodes. The ROIs drawn on the CT images of each patient were transferred to the co-registered PET images and the amount of [¹⁸F]FDG pathological uptake was calculated for each ROI, determining maximum, peak, and minimum SUVs, normalized by body weight (SUV_{max}, SUV_{peak}, and SUV_{min}, respectively) and lean body mass (SUL); metabolic tumoral volume (MTV; volume of pixels in the ROI with SUV_{max} >40%); and total lesion glycolysis (TLG; MTV multiplied by SUV_{mean}).

2.6. Chest CT and X-ray Image Interpretation

Upon their diagnosis, all patients underwent chest X-ray in posterior-anterior and lateral projections, reported by specialist radiologists according to current recommenda-

tions [16,17]. They characterized the density (alveolar, ground glass, or mixed), distribution (central, peripheral, or diffuse), location (unilateral or bilateral), and extent (unilobar or multilobar).

2.7. Statistical Analysis

All measurements for each participant were independently conducted by two nuclear medicine physicians, considering the mean value in statistical analyses. Absolute numbers and percentages were calculated for categorical variables and means with standard deviation (SD) for continuous variables. For comparisons of quantitative data between the positive and negative PET groups, the Student's *t*-test was applied when the distribution was normal and the Mann–Whitney U test when it was not. Associations with categorical variables were evaluated by constructing contingency tables, applying the chi-square test for individual comparisons and Fisher's exact test for multiple comparisons. Volumetric [¹⁸F]FDG-PET/CT results were correlated with laboratory test results and respiratory function parameters by using Spearman's rank correlation coefficient. IBM SPSS version 15.0 (IBM Corp, Armonk, NY, USA) and R software were used for statistical analyses. A $p \leq 0.05$ was considered significant in all tests.

3. Results

The study included 20 patients (60% males) with a mean age of 55.85 ± 9.28 years admitted for pneumonia and/or respiratory failure between 27 November 2020 and 1 March 2021 (during the "third wave" of COVID-19 in Spain). The mean hospital stay was 16.70 ± 11.99 days. Table 1 summarizes the baseline characteristics of the patients.

Table 1. Baseline clinical characteristics and risk factors of patients.

Clinical Characteristics (<i>n</i>)	Mean \pm SD or <i>n</i> (%)
Age (years)	55.85 \pm 9.28
Gender (Male)	12 (60)
BMI (kg/m ²)	34.11 \pm 7.23
Comorbidities	
Former or current smoking habit	2 (10)
Hypertension	5 (25)
Diabetes	3 (15)
Hyperlipidemia	2 (10)
Atrial fibrillation	2 (10)
Asthma	3 (15)
Charlson Comorbidity index	1.60 \pm 1.14
Charlson Comorbidity index \geq 2	9 (45)
Clinical characteristics at admission	
Fever	17 (85)
Dyspnea	15 (75)
Irritative cough	16 (80)
Fatigue	14 (70)
Myalgia	11 (55)
Anosmia/Ageusia	2 (10)
Digestive symptoms	9 (45)
Headache	3 (15)
ARDS (PaO ₂ /FIO ₂ < 300 mmHg)	14 (70)
Blood oxygen saturation	90.90 \pm 5.33

Table 1. *Cont.*

Clinical Characteristics (<i>n</i>)	Mean ± SD or <i>n</i> (%)
Laboratory test results at admission	
Hemoglobin (g/dL)	14.86 ± 1.84
White blood cell (count × 10 ³ /μL)	7.68 ± 3.11
Neutrophil (count × 10 ³ /μL)	6.28 ± 3.16
Lymphocyte (count × 10 ³ /μL)	0.99 ± 0.57
NLR	8.36 ± 5.86
Platelet (count × 10 ³ /μL)	206.65 ± 54.49
Ferritin (ng/mL)	1327.81 ± 1402.58
C-reactive protein (mg/L)	81.20 ± 54.61
LDH (U/L)	398.15 ± 113.80
AST(U/L)	49.25 ± 38.60
ALT(U/L)	48.30 ± 46.36
Albumin (g/dL)	3.92 ± 0.50
D-dimer (mg/L)	0.73 ± 0.52
Characteristics of Hospitalization	
Hospital stay (days)	16.70 ± 11.99
Pneumonia (chest X-ray)	19 (95)
ICU admission	10 (50)
Invasive mechanical ventilation	5 (25)
Bolus therapy with glucocorticoid	14 (60)
Antiviral therapy	5 (25)
Selective inhibitors of pro-inflammatory cytokines	6 (30)

Continuous variables are presented as means ± standard deviation (SD) and categorical variables as frequencies (percentages). ARDS: acute respiratory distress syndrome; AST: aspartate aminotransferase; ALT: alanine transaminase; NLR: neutrophil/lymphocyte ratio; PCT: procalcitonin; NT-proBNP: N terminal pro-B-type natriuretic peptide; LDH: lactate dehydrogenase; ICU: intensive care unit.

The main symptom at admission was fever in 17/20 patients (85%), followed by irritative cough in 16 (80%), dyspnea in 15 (75%), fatigue in 14 (70%), and ageusia and/or anosmia in 2 patients (10%). Chest X-ray findings compatible with pneumonia were observed in 19 patients (95%), being multilobar in 18 (97.4%) and unilobar in 1 (5.3%). The radiological pattern was alveolar in three patients (15.8%), ground glass in seven (36.8%), and mixed in the remaining nine (47.4%). The main associated complication during hospitalization was respiratory distress in 14 (70%) patients; admission to the intensive care unit (ICU) was required for seven (35%) of these patients and invasive mechanical ventilation in five (25%). All patients were treated with corticosteroids, administered as a bolus in 14 patients (70%). Five patients (25%) received antiviral treatment and another six (30%) were treated with selective inhibitors of pro-inflammatory cytokines (five with tocilizumab and one with anakinra). Finally, three patients (15%) required home oxygen therapy at discharge.

3.1. The [¹⁸F]FDG-PET/CT Findings

The mean time from hospital discharge to [¹⁸F]FDG-PET/CT study was 58.85 ± 13.67 days. The result was positive in 11 patients (55%) and negative in 9 (45%). The main finding was hypermetabolic lymphadenopathy in the mediastinum, observed in 10 (90.9%) of the [¹⁸F]FDG-PET/CT-positive patients (Figure 1).

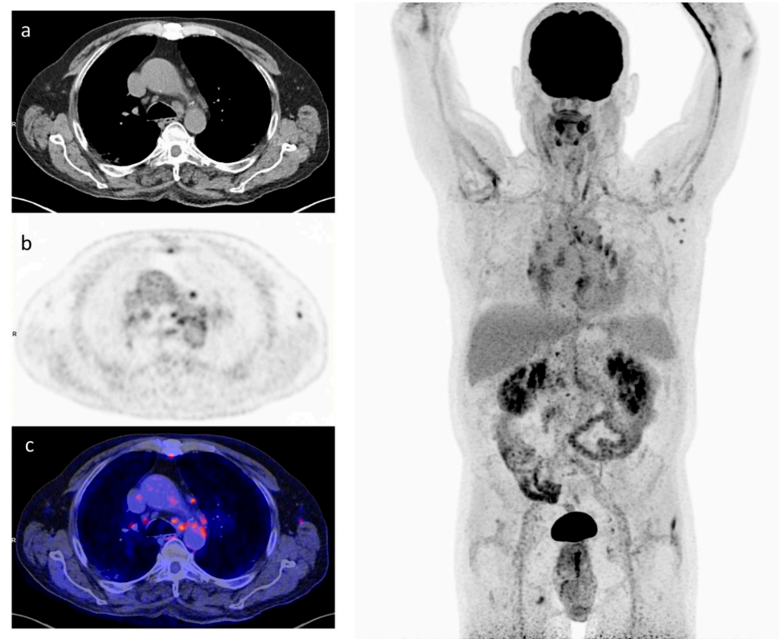


Figure 1. A 64-year man admitted for multilobar pneumonia caused by SARS-CoV-2. The [¹⁸F]FDG-PET/CT at 3 months after symptom onset shows increased [¹⁸F]FDG uptake in residual pulmonary lesions (TLG 124,11) and mediastinum lymph node (SUVpeak 1,73). Pulmonary function tests evidenced severe pulmonary diffusion impairment, with a diffusing capacity of the lungs for carbon monoxide 41% of the predicted value. Left: (a) CT transverse slice, (b) [¹⁸F]FDG-PET slice, and (c) fused [¹⁸F]FDG-PET and CT images. Right: whole-body, maximal intensity projection image, displaying mediastinal lymph nodes with [¹⁸F]FDG uptake.

Patients with positive and negative [¹⁸F]FDG-PET/CT results significantly differed in age (59.82 ± 8.52 vs. 51.00 ± 8.09 years, respectively, $p = 0.03$), Charlson index score ≥ 1 (66.7 vs. 100%, $p = 0.038$), presence of fatigue (90.9 vs. 44.4%, $p = 0.024$) and respiratory distress (90.9 vs. 44.4%, $p = 0.024$), hemoglobin levels (13.41 ± 1.91 vs. 15.24 ± 1.58 g/dL, $p = 0.041$), and lymphocyte count (1.78 ± 0.53 vs. $2.47 \pm 0.49 \times 10^3/\mu\text{L}$, $p = 0.011$) at 2–3 months post-discharge (Figure 2).

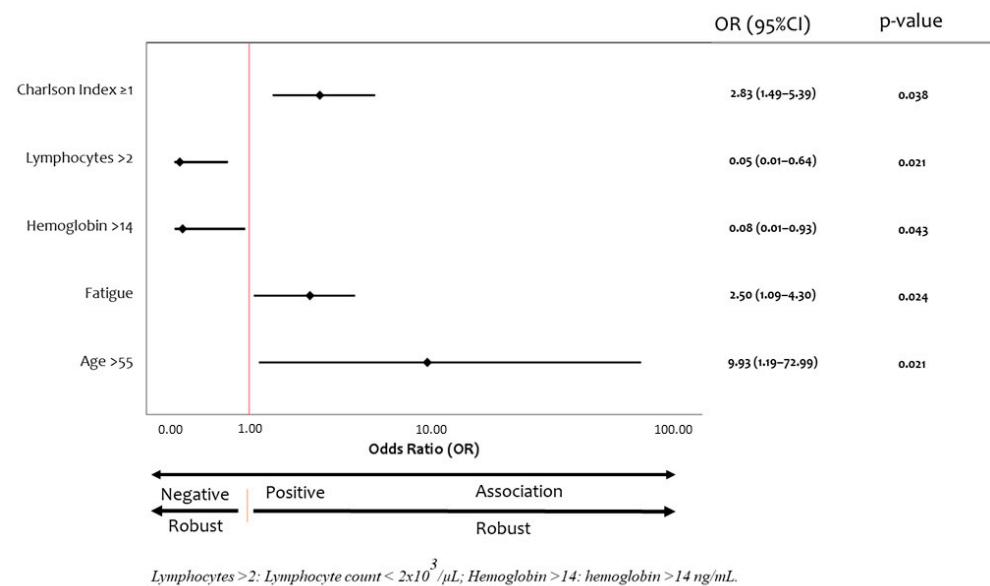


Figure 2. Factors associated with [¹⁸F]FDG-PET/CT positive. Forest plot with odds ratios shown by closed circles and 95% confidence intervals by whiskers.

3.2. Correlation of Volumetric [¹⁸F]FDG-PET/CT Parameters with Laboratory Test Results

Table 2 exhibits associations observed between volumetric [¹⁸F]FDG-PET/CT results and analytical findings at admission, during the hospital stay, and at 2–3 months post-discharge.

Table 2. Bivariate correlations of volumetric [¹⁸F]FDG PET/CT parameters with laboratory parameters at admission, during hospital stay, and at 2–3 months post-discharge (short-term follow-up).

	Variable	SUVPeak		Pulmonary TLG	
		Spearman's rho	p-Value	Spearman's rho	p-Value
Admission	Hemoglobin (g/dL)	−0.664	0.026		
	Neutrophil count	−0.764	0.006		
	Lymphocyte count	0.636	0.035		
	NLR	−0.664	0.026		
Hospital stay	Neutrophil count	−0.700	0.016		
	Lymphocyte count	0.618	0.043		
	NLR	−0.627	0.039		
	IL-6			0.624	0.010
	C-reactive protein			0.618	0.004
	PCT			0.570	0.049
	LDH			0.445	0.049
	Troponin			0.883	0.002
	Fibrinogen			0.635	0.015
	D-dimer			0.674	0.001
Short-term follow-up	Neutrophil count	−0.679	0.022		
	Lymphocyte count	0.791	0.004		
	NLR	−0.727	0.011		

IL-6: interleukin 6; LDH: lactate dehydrogenase; NLR: neutrophil/lymphocyte ratio; PCT: procalcitonin.

At admission, a significant correlation was found between the SUVpeak of the target lesion in the mediastinum and the hemoglobin level ($r = 0.615$, $p = 0.044$), leukocyte count ($\rho = -0.664$, $p = 0.026$), neutrophil count ($\rho = -0.764$, $p = 0.006$), lymphocyte count ($\rho = 0.636$, $p = 0.035$), and NLR ($\rho = -0.664$, $p = 0.026$). In addition, the TLG in lung parenchyma was significantly correlated with C-reactive protein (CRP) ($\rho = 0.558$, $p = 0.011$), procalcitonin ($\rho = 0.611$, $p = 0.035$), fibrinogen ($\rho = 0.472$, $p = 0.041$), and blood glucose ($\rho = 0.517$, $p = 0.020$) levels at hospital admission.

During hospitalization, the SUVpeak of the target lesion was again significantly correlated with neutrophil count ($\rho = -0.700$, $p = 0.016$), lymphocyte count ($\rho = 0.618$, $p = 0.043$), and NLR ($\rho = -0.627$, $p = 0.039$). Furthermore, pulmonary TLG was significantly correlated with IL-6 ($\rho = 0.624$, $p = 0.010$), CRP ($\rho = 0.618$, $p = 0.004$), procalcitonin ($\rho = 0.570$, $p = 0.042$), LDH ($\rho = 0.445$, $p = 0.049$), troponin ($\rho = 0.883$, $p = 0.002$), fibrinogen ($\rho = 0.635$, $p = 0.015$), and D-dimer ($\rho = 0.674$, $p = 0.001$) levels and with the neutrophil count ($\rho = 0.615$, $p = 0.044$), lymphocyte count ($\rho = -0.615$, $p = 0.004$), and NLR ($\rho = 0.558$, $p = 0.011$) during the hospital stay.

At the follow-up at 2–3 months, the SUVpeak was significantly correlated with neutrophil count ($\rho = -0.679$, $p = 0.022$), lymphocyte count ($\rho = 0.791$, $p = 0.004$), and NLR ($\rho = -0.727$, $p = 0.011$). No significant correlation was found between pulmonary TLG and any analytical parameter under study (Figure 3).

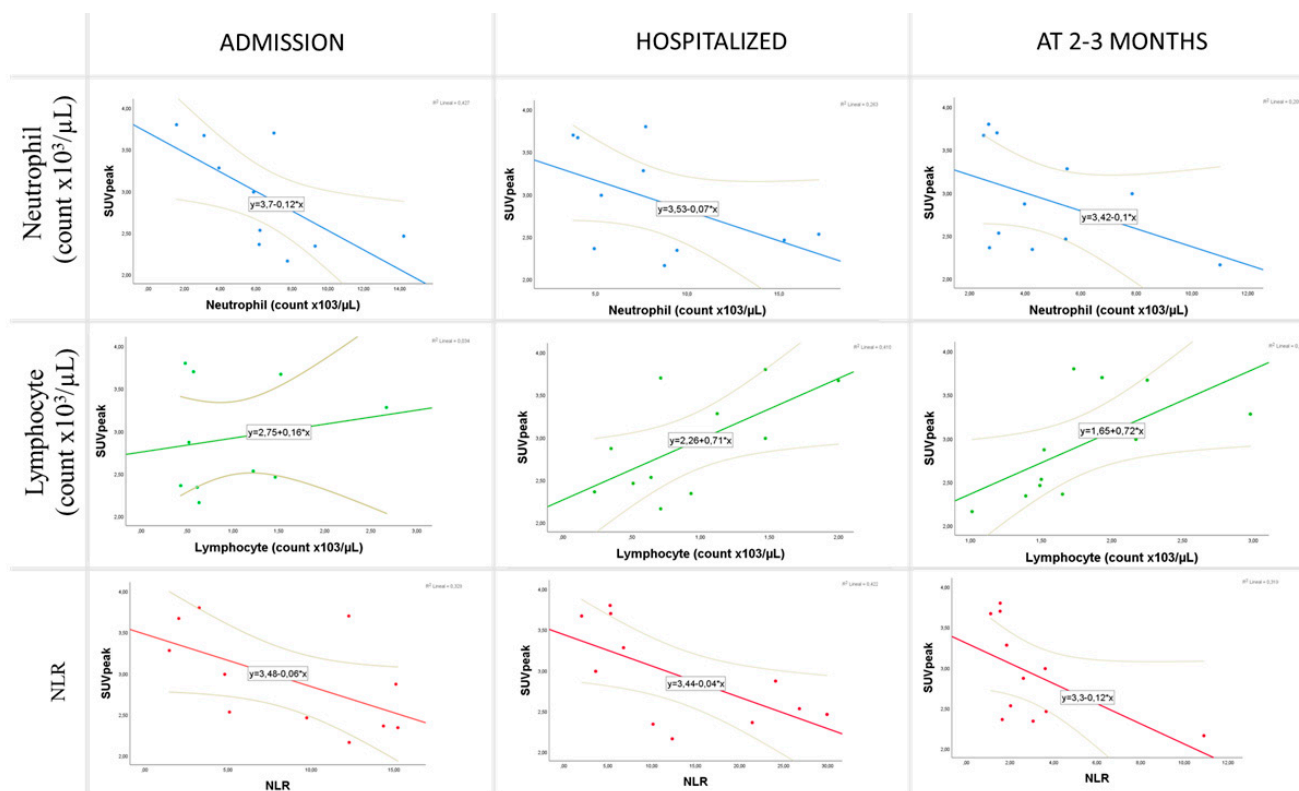


Figure 3. Scatter plot matrix. Correlation of the SUVpeak of the target lesion with neutrophil and lymphocyte counts and NLR at admission, during hospital stay, and at 2–3 months post-discharge.

3.3. Correlation of Volumetric ¹⁸F]FDG-PET/CT Parameters with Respiratory Function Parameters

Eleven (55%) of the 20 patients had impaired respiratory function. Percentage predicted values were <80% for FVC in 20% of patients, <80% for FEV1 in 15%, <70% for FEV1/FVC in 5%, <80% for TLC in 20%, <80 for DLCO in 35%, <80% for KCO in 25%, and <65% for VR in 5%. Saturation was ≥4% lower at the finish versus start of the walk test in four patients (20%), and the distance was <400 m in three (15%).

Volumetric ¹⁸F]FDG-PET/CT parameters were related to respiratory function test results obtained at 2–3 months post-discharge (Figure 4). The SUVpeak of the target lesion in the mediastinum was significantly and positively correlated with % predicted DLCO (rho = 0.782, p = 0.008), KCO (rho = 0.721, p = 0.019), and RV (rho = 0.636, p = 0.048) values. Pulmonary TLG was significantly and negatively correlated with % predicted DLCO (rho = −0.628, p = 0.005), KCO (rho = −0.564, p = 0.014), TLC (rho = −0.532, p = 0.023), and RV (rho = −0.554, p = 0.017) values. (Table 3).

Table 3. Bivariate correlations of volumetric ¹⁸F]FDG PET/CT parameters and respiratory function parameters in the short-term follow-up.

Variable	SUVpeak		Pulmonary TLG	
	Spearman’s rho	p-Value	Spearman’s rho	p-Value
DLCO% pred	0.782	0.008	−0.628	0.005
KCO% pred	0.721	0.019	−0.564	0.014
TLC% pred	0.467	0.174	−0.532	0.023
RV% pred	0.636	0.048	−0.554	0.017

DLCO: diffusing capacity of the lungs for carbon monoxide; KCO: CO transfer coefficient; RV: residual volume; TLC: total lung capacity.

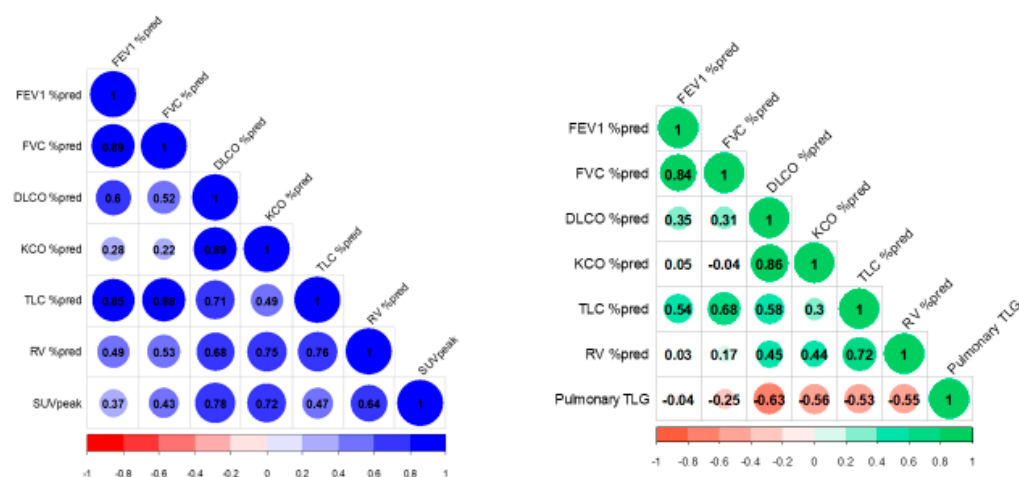


Figure 4. Correlogram showing the association of respiratory function test results with the SUVpeak of the target lesion and pulmonary TLG.

4. Discussion

In this study, [^{18}F]FDG-PET/CT was used to measure the metabolism of lungs and other organs in the short–medium follow-up of patients admitted to hospital for pneumonia or respiratory failure due to COVID-19 infection. Despite testing negative for the infection in two successive RT-PCR tests of nasopharyngeal swabs, more than half of the patients showed increased metabolic activity (i.e., persistent inflammation) on [^{18}F]FDG-PET/CT images in lung tissue of normal appearance and in mediastinal lymph nodes. To our best knowledge, [^{18}F]FDG-PET/CT has not previously been used to detect residual inflammatory processes after COVID-19 infection. These findings contribute evidence on the pathophysiological processes in patients who survive hospital admission for COVID-19 pneumonia.

The [^{18}F]FDG-PET/CT has been employed in patients with influenza A, aspiration pneumonia, and organized pneumonia to assess the extent and severity of the disease, to follow its course, and to evaluate the response to therapy [5,18,19]. Research on the role of [^{18}F]FDG-PET/CT in COVID-19 infection has generally focused on the acute phase. In this regard, Qin et al. reported high [^{18}F]FDG uptake in lung lesions and mediastinal lymph nodes of four patients strongly suspected of the infection [4], and Colandrea et al. described elevated [^{18}F]FDG uptake in lung lesions in 80% of a series of symptom-free oncology patients diagnosed with COVID-19 [20]. However, few studies have addressed the short- or medium-term consequences of COVID-19 infection. Dietz et al. recently reported increased [^{18}F]FDG uptake in lung lesions and mediastinal lymph nodes of 13 non-critically ill COVID-19 patients at days 6–14 after symptom onset, although the short-axis diameter of mediastinal lymph nodes was always < 1 cm [3]. Johnson et al. proposed that high [^{18}F]FDG uptake in mediastinal lymph nodes might be secondary to lung involvement in COVID-19 [21]. Bai et al. found elevated metabolic activity in residual lung lesions in COVID-19 survivors after two successive negative results in the RT-PCR test [22], and Scarlattei et al. reported that this metabolic activity remained high many weeks after the disappearance of symptoms and a negative RT-PCR test result [23]. The present results are in line with the above findings and contribute novel data on increased metabolic activity in lung tissue of normal appearance and in mediastinal lymph nodes of normal size. In this context, Xu et al. described lymphocyte-dominated interstitial mononuclear inflammatory infiltrates in both lungs of a patient with COVID-19 and reported that substantial inflammation may persist in the lungs after the disappearance of the infection [24]. The elevated [^{18}F]FDG uptake would reflect increased glycolytic activity due to infiltration and inflammation of the lung, even in normally aerated areas that show no morphological alterations on CT images, demonstrating the greater capacity of [^{18}F]FDG-PET/CT to detect inflamed lung areas in comparison to CT alone [8,22], which

may persist long after the disappearance of COVID-19 infection. The possible duration of the post-COVID-19 inflammatory response in lungs and extrapulmonary sites has yet to be established and warrants further research.

At 2–3 months post-discharge, patients with elevated chest [^{18}F]FDG uptake were older and characterized by a higher Charlson index, more frequent fatigue and respiratory distress, and lower hemoglobin and lymphocyte counts in comparison to those with normal [^{18}F]FDG uptake. The SUV_{peak} of the target lesion and pulmonary TLG were significantly correlated with acute phase reactants and white blood cell counts at admission, during the hospital stay, and at 2–3 months post-discharge. Although there is a lack of similar studies in severely ill COVID-19 survivors for comparison with these results, they are consistent with previous findings on risk factors for more severe infection, including old age, underlying comorbidities [12,25], and similar changes in white blood cell counts, lymphocyte counts, procalcitonin and CRP levels, and NLR [26,27]. The [^{18}F]FDG-PET/CT findings were correlated with the NLR in all studied phases of COVID-19 disease. The persistence over time of increased [^{18}F]FDG uptake intensity may reflect a more severe acute phase of the disease.

The lung appears to be the most frequently involved organ in COVID-19, with reports of diffuse alveolar epithelium destruction, capillary damage/bleeding, hyaline membrane formation, alveolar septal fibrous proliferation, and/or pulmonary consolidation, among others [12,24]. Long-term follow-up studies of survivors of other coronavirus infections found that respiratory function limitations frequently last for months or even years, including impaired DLCO (in 15.5–43.6% of patients) and decreased TLC (5.2–10.9%) [28–30]. Various authors have addressed short- and medium-term respiratory function outcomes in survivors of COVID-19 infection, usually at hospital discharge [31,32]. In a study at 2–3 months post-discharge of 55 COVID-19 survivors who had not required mechanical ventilation, Zhao et al. described residual pulmonary function in 14 patients (25.45%), mainly impaired DLCO (in 13.6%) [33]. In a study at 6 weeks post-discharge of 124 COVID-19 survivors, van den Borst et al. [34] described an improvement in radiological images for almost all patients (99%) but observed residual lung parenchymal alterations in 91% of the patients and reduced lung diffusion capacity in 42%. Likewise, in their study at 3 months post-discharge of 76 healthcare workers who recovered from COVID-19, Liang et al. reported normal FEV₁, FVC, FEV₁/FVC, TLC, and DLCO values (>80% predicted) in 82% of the patients but the persistence of mild pulmonary function abnormalities in 42% [35]. The proportion of the present patients with impaired pulmonary function at 2–3 months was in line with previous findings on the short- to medium-term effects of COVID-19 infection [33,34].

The most frequent respiratory sequela of COVID-19 was DLCO alteration, as reported in previous studies, which may indicate the presence of pulmonary fibrosis [12,24]. DLCO and other respiratory function parameters were negatively correlated with the lung [^{18}F]FDG uptake as quantified by TLG. Although only a small proportion of the present patients had severe airway dysfunction, the results suggest that COVID-19 produces diffuse pulmonary epithelial damage and mild congestion of the airway mediated by lymphocyte-dominated interstitial inflammatory infiltrates. No published data appear to be available on the association between respiratory function test results and pulmonary TLG. The majority of the present patients showed no lung lesions on CT scans at 2–3 months after discharge; however, pulmonary function was impaired in more than half of the patients with a normal lung CT scan. Hence, pulmonary function and [^{18}F]FDG-PET/CT testing is more sensitive than CT alone for identifying candidates for pulmonary rehabilitation after SARS-CoV-2 pneumonia [22].

High [^{18}F]FDG uptake may be related to increased anaerobic glycolysis caused by a cascade of reactions involving inflammatory cells [7,36]. In this way, the uptake of [^{18}F]FDG by lung lesions and lymph nodes observed in this study may be due to nonspecific immune or inflammatory activation, similar to the high [^{18}F]FDG uptake observed in lung lesions

caused by the Middle East respiratory syndrome, pandemic H1N1 influenza virus, and organized pneumonia [18,19,37].

The [^{18}F]FDG-PET/CT offers a complementary approach to other imaging modalities by providing metabolic information. Although not currently recommended for the diagnosis of COVID-19 in the acute phase [8], it can yield relevant information for the diagnosis of short- and medium-term complications, including the chronic damage to the lungs and extrapulmonary sites that can follow acute infection [6,22]. However, radiologists and nuclear physicians need to develop a thorough understanding of the cellular mechanisms that underlie the pathophysiology of COVID-19 in the clinical settings of lung and extrapulmonary malignancies and inflammatory diseases in order to avoid misinterpretation of [^{18}F]FDG-PET/CT images [31].

Besides the small sample size, the main limitation of this study was the absence of a control group, hampering the possibility to detect causal relationships between the findings and COVID-19 infection. The epidemiological environment in which this study was carried out determined strict, restrictive conditions for access to hospital centers in our center and population. Evidently, the performance of [^{18}F]PET/CT in healthy collaborating patients was obviously not authorized. In addition, no test results were available for the baseline respiratory function of patients before COVID-19, although the presence of chronic lung disease was an exclusion criterion. Further research is required to fully elucidate the impact of COVID-19 on pulmonary function. In this regard, the present results cannot be extrapolated to patients with chronic lung disease. Another study limitation was the absence of a follow-up period to explore the long-term clinical relevance of the respiratory function impairment. Finally, biopsy specimens were not available for the studied organs. Nevertheless, the present findings contribute to laying the foundations for future studies with larger series on the potential role of [^{18}F]FDG-PET/CT in evaluating the sequelae of COVID-19 infection. These should have prolonged follow-up periods to explore the possible relationship between initial lung inflammation and long-term sequelae such as residual lung fibrosis and respiratory failure.

5. Conclusions

In conclusion, at 2–3 months after the acute phase of SARS-CoV-2 infection, almost half of the patients evidenced an impairment of pulmonary function that was correlated with [^{18}F]FDG-PET/CT findings. In addition, the increased metabolic activity observed in the lung and mediastinal lymph node was associated with clinical and laboratory markers of disease severity. The [^{18}F]FDG-PET/CT is useful to obtain novel information on the pathogenesis of COVID-19 and on the diagnostic and evaluation of short- and medium-term sequelae, contributing to their management.

Author Contributions: E.M.T.-I., T.R.-S. and B.M.J.-R. contributed to collecting data, manuscript preparation/editing, and literature research; E.M.T.-I., B.M.J.-R., E.Y.G.-R., A.R.-F., J.M.L.-E., T.R.-S., M.G.-R. and C.M.-G. contributed to the study concept and design; E.M.T.-I. and B.M.J.-R. contributed to data analysis and interpretation and for manuscript editing; M.G.-R., J.M.L.-E. and C.M.-G. contributed to study design/planning and final approval. All authors have read and agreed to the published version of the manuscript.

Funding: This research received no external funding.

Institutional Review Board Statement: The study was conducted in accordance with the Declaration of Helsinki and approved by the Institutional Review Board (or Ethics Committee) of Hospital Universitario Virgen de las Nieves (protocol code 1444-N-21).

Informed Consent Statement: Informed consent was obtained from all subjects involved in the study. Written informed consent has been obtained from the patient(s) to publish this paper.

Acknowledgments: This research is associated with the doctoral thesis of Beatriz María Jiménez Rodríguez under the Clinical Medicine and Public Health Doctorate Program of the University of Granada.

Conflicts of Interest: All authors declare that they do not have conflicts of financial or non-financial interest. Written consent was obtained for all patients and a local ethics committee approved the study.

References

- Chen, N.; Zhou, M.; Dong, X.; Qu, J.; Gong, F.; Han, Y.; Qiu, Y.; Wang, J.; Liu, Y.; Wei, Y.; et al. Epidemiological and clinical characteristics of 99 cases of 2019 novel coronavirus pneumonia in Wuhan, China: A descriptive study. *Lancet* **2020**, *395*, 507–513. [CrossRef]
- Chung, M.; Bernheim, A.; Mei, X.; Zhang, N.; Huang, M.; Zeng, X.; Cui, J.; Xu, W.; Yang, Y.; Fayad, Z.A.; et al. CT Imaging Features of 2019 Novel Coronavirus (2019-nCoV). *Radiology* **2020**, *295*, 202–207. [CrossRef] [PubMed]
- Dietz, M.; Chironi, G.; Claessens, Y.E.; Farhad, R.L.; Rouquette, I.; Serrano, B.; Nataf, V.; Hugonnet, F.; Paulmier, B.; Berthier, F.; et al. COVID-19 pneumonia: Relationship between inflammation assessed by whole-body FDG PET/CT and short-term clinical outcome. *Eur. J. Nucl. Med. Mol. Imaging* **2021**, *48*, 260–268. [CrossRef] [PubMed]
- Qin, C.; Liu, F.; Yen, T.C.; Lan, X. 18F-FDG PET/CT findings of COVID-19: A series of four highly suspected cases. *Eur. J. Nucl. Med. Mol. Imaging* **2020**, *47*, 1281–1286. [CrossRef] [PubMed]
- Capitano, S.; Nordin, A.J.; Noraini, A.R.; Rossetti, C. PET/CT in nononcological lung diseases: Current applications and future perspectives. *Eur. Respir. Rev.* **2016**, *25*, 247–258. [CrossRef] [PubMed]
- Lütje, S.; Marinova, M.; Kütting, D.; Attenberger, U.; Essler, M.; Bundschuh, R.A. Nuclear medicine in SARS-CoV-2 pandemia: 18F-FDG-PET/CT to visualize COVID-19. *Nuklearmedizin* **2020**, *59*, 276–280. [CrossRef] [PubMed]
- Annunziata, S.; Delgado Bolton, R.C.; Kamani, C.H.; Prior, J.O.; Albano, D.; Bertagna, F.; Treglia, G. Role of 2-[18F]FDG as a Radiopharmaceutical for PET/CT in Patients with COVID-19: A Systematic Review. *Pharmaceuticals* **2020**, *13*, 377. [CrossRef]
- Jin, C.; Luo, X.; Qian, S.; Zhang, K.; Gao, Y.; Zhou, R.; Cen, P.; Xu, Z.; Zhang, H.; Tian, M. Positron emission tomography in the COVID-19 pandemic era. *Eur. J. Nucl. Med. Mol. Imaging* **2021**, *48*, 1–15. [CrossRef]
- Mucientes, J.; Calles, L.; Rodríguez, B.; Mitjavila, M. Parameters of metabolic quantification in clinical practice. Is it now time to include them in reports? *Rev. Española De Med. Nucl. E Imagen Mol.* **2018**, *37*, 264–270. [CrossRef]
- Clinical Management of Severe Acute Respiratory Infection When Novel Coronavirus (nCoV) Infection Is Suspected [Internet]. Available online: <https://www.who.int/publications/i/item/10665-332299> (accessed on 2 February 2022).
- Paez, D.; Gnanasegaran, G.; Fanti, S.; Bomanji, J.; Hacker, M.; Sathekge, M.; Bom, H.S.; Cerci, J.J.; Chiti, A.; Herrmann, K.; et al. COVID-19 pandemic: Guidance for nuclear medicine departments. *Eur. J. Nucl. Med. Mol. Imaging* **2020**, *47*, 1615–1619. [CrossRef]
- Zhou, F.; Yu, T.; Du, R.; Fan, G.; Liu, Y.; Liu, Z.; Xiang, J.; Wang, Y.; Song, B.; Gu, X.; et al. Clinical course and risk factors for mortality of adult inpatients with COVID-19 in Wuhan, China: A retrospective cohort study. *Lancet* **2020**, *395*, 1054–1062. [CrossRef]
- Graham, B.L.; Brusasco, V.; Burgos, F.; Cooper, B.G.; Jensen, R.; Kendrick, A.; MacIntyre, N.R.; Thompson, B.R.; Wanger, J. 2017 ERS/ATS standards for single-breath carbon monoxide uptake in the lung. *Eur. Respir. J.* **2017**, *49*, 1600016, Erratum in *Eur. Respir. J.* **2018**, *52*. [CrossRef] [PubMed]
- García-Río, F.; Calle, M.; Burgos, F.; Casan, P.; Del Campo, F.; Galdiz, J.B.; Giner, J.; González-Mangado, N.; Ortega, F.; Puente Maestu, L. Spanish Society of Pulmonology and Thoracic Surgery (SEPAR). Spirometry. Spanish Society of Pulmonology and Thoracic Surgery (SEPAR). *Arch. Bronconeumol.* **2013**, *49*, 388–401. [CrossRef]
- García Garzón, J.R.; Rodríguez, A.; Cabrera, A. Tomografía por emisión de positrones de cuerpo completo (PET/TAC) con 18F-fluorodesoxiglucosa. Grupo de Trabajo PET, Comité de Procedimientos de la SEMN [Positron emission tomography/computed tomography with 18F-FDG. PET Working Group. Procedures Committee of the Spanish Society of Nuclear Medicine]. *Rev. Española De Med. Nucl.* **2009**, *28*, 85–89. (In Spanish) [CrossRef]
- Hansell, D.M.; Bankier, A.A.; MacMahon, H.; McLoud, T.C.; Müller, N.L.; Remy, J. Fleischner Society: Glossary of terms for thoracic imaging. *Radiology* **2008**, *246*, 697–722. [CrossRef]
- Salehi, S.; Abedi, A.; Balakrishnan, S.; Gholamrezanezhad, A. Coronavirus Disease 2019 (COVID-19): A Systematic Review of Imaging Findings in 919 Patients. *AJR Am. J. Roentgenol.* **2020**, *215*, 87–93. [CrossRef]
- Jonsson, C.B.; Camp, J.V.; Wu, A.; Zheng, H.; Kraenzle, J.L.; Biller, A.E.; Vanover, C.D.; Chu, Y.K.; Ng, C.K.; Proctor, M.; et al. Molecular imaging reveals a progressive pulmonary inflammation in lower airways in ferrets infected with 2009 H1N1 pandemic influenza virus. *PLoS ONE* **2012**, *7*, e40094. [CrossRef]
- Chefer, S.; Thomasson, D.; Seidel, J.; Reba, R.C.; Bohannon, J.K.; Lackemeyer, M.G.; Bartos, C.; Sayre, P.J.; Bollinger, L.; Hensley, L.E.; et al. Modeling [(18)F]-FDG lymphoid tissue kinetics to characterize nonhuman primate immune response to Middle East respiratory syndrome-coronavirus aerosol challenge. *EJNMMI Res.* **2015**, *5*, 65. [CrossRef]
- Colandrea, M.; Gilardi, L.; Travaini, L.L.; Fracassi, S.L.V.; Funicelli, L.; Grana, C.M. 18F-FDG PET/CT in asymptomatic patients with COVID-19: The submerged iceberg surfaces. *Jpn. J. Radiol.* **2020**, *38*, 1007–1011. [CrossRef]
- Johnson, L.N.; Vesselle, H. COVID-19 in an asymptomatic patient undergoing FDG PET/CT. *Radiol. Case Rep.* **2020**, *15*, 1809–1812. [CrossRef]
- Bai, Y.; Xu, J.; Chen, L.; Fu, C.; Kang, Y.; Zhang, W.; Fakhri, G.E.; Gu, J.; Shao, F.; Wang, M. Inflammatory response in lungs and extrapulmonary sites detected by [18F] fluorodeoxyglucose PET/CT in convalescing COVID-19 patients tested negative for coronavirus. *Eur. J. Nucl. Med. Mol. Imaging* **2021**, *48*, 2531–2542. [CrossRef]

23. Scarlattei, M.; Baldari, G.; Silva, M.; Bola, S.; Sammartano, A.; Migliari, S.; Graziani, T.; Cidda, C.; Sverzellati, N.; Ruffini, L. Unknown SARS-CoV-2 pneumonia detected by PET/CT in patients with cancer. *Tumori J.* **2020**, *106*, 325–332. [[CrossRef](#)]
24. Xu, Z.; Shi, L.; Wang, Y.; Zhang, J.; Huang, L.; Zhang, C.; Liu, S.; Zhao, P.; Liu, H.; Zhu, L.; et al. Pathological findings of COVID-19 associated with acute respiratory distress syndrome. *Lancet Respir. Med.* **2020**, *8*, 420–422. [[CrossRef](#)]
25. Gao, Y.D.; Ding, M.; Dong, X.; Zhang, J.J.; Kursat Azkur, A.; Azkur, D.; Gan, H.; Sun, Y.L.; Fu, W.; Li, W.; et al. Risk factors for severe and critically ill COVID-19 patients: A review. *Allergy* **2021**, *76*, 428–455. [[CrossRef](#)]
26. Feng, X.; Li, S.; Sun, Q.; Zhu, J.; Chen, B.; Xiong, M.; Cao, G. Immune-Inflammatory Parameters in COVID-19 Cases: A Systematic Review and Meta-Analysis. *Front. Med.* **2020**, *7*, 301. [[CrossRef](#)]
27. Sayah, W.; Berkane, I.; Guermache, I.; Sabri, M.; Lakhal, F.Z.; Rahali, S.Y.; Djidjeli, A.; Merah, F.; Belaid, B.; Berkani, L.; et al. Interleukin-6, procalcitonin and neutrophil-to-lymphocyte ratio: Potential immune-inflammatory parameters to identify severe and fatal forms of COVID-19. *Cytokine* **2021**, *141*, 155428. [[CrossRef](#)]
28. Hui, D.S.; Joynt, G.M.; Wong, K.T.; Gomersall, C.D.; Li, T.S.; Antonio, G.; Ko, F.W.; Chan, M.C.; Chan, D.P.; Tong, M.W.; et al. Impact of severe acute respiratory syndrome (SARS) on pulmonary function, functional capacity and quality of life in a cohort of survivors. *Thorax* **2005**, *60*, 401–409. [[CrossRef](#)]
29. Ngai, J.C.; Ko, F.W.; Ng, S.S.; To, K.W.; Tong, M.; Hui, D.S. The long-term impact of severe acute respiratory syndrome on pulmonary function, exercise capacity and health status. *Respirology* **2010**, *15*, 543–550. [[CrossRef](#)]
30. Park, W.B.; Jun, K.I.; Kim, G.; Choi, J.P.; Rhee, J.Y.; Cheon, S.; Lee, C.H.; Park, J.S.; Kim, Y.; Joh, J.S.; et al. Correlation between Pneumonia Severity and Pulmonary Complications in Middle East Respiratory Syndrome. *J. Korean Med. Sci.* **2018**, *33*, e169. [[CrossRef](#)]
31. Mo, X.; Jian, W.; Su, Z.; Chen, M.; Peng, H.; Peng, P.; Lei, C.; Chen, R.; Zhong, N.; Li, S. Abnormal pulmonary function in COVID-19 patients at time of hospital discharge. *Eur. Respir. J.* **2020**, *55*, 2001217. [[CrossRef](#)]
32. You, J.; Zhang, L.; Ni-Jia-Ti, M.Y.; Zhang, J.; Hu, F.; Chen, L.; Dong, Y.; Yang, K.; Zhang, B.; Zhang, S. Anormal pulmonary function and residual CT abnormalities in rehabilitating COVID-19 patients after discharge. *J. Infect.* **2020**, *81*, e150–e152. [[CrossRef](#)] [[PubMed](#)]
33. Zhao, Y.M.; Shang, Y.M.; Song, W.B.; Li, Q.Q.; Xie, H.; Xu, Q.F.; Jia, J.L.; Li, L.M.; Mao, H.L.; Zhou, X.M.; et al. Follow-up study of the pulmonary function and related physiological characteristics of COVID-19 survivors three months after recovery. *EClinicalMedicine* **2020**, *25*, 100463. [[CrossRef](#)] [[PubMed](#)]
34. van den Borst, B.; Peters, J.B.; Brink, M.; Schoon, Y.; Bleeker-Rovers, C.P.; Schers, H.; van Hees, H.W.; van Helvoort, H.; van den Boogaard, M.; van der Hoeven, H.; et al. Comprehensive health assessment three months after recovery from acute COVID-19. *Clin. Infect. Dis.* **2020**, *73*, e1089–e1098. [[CrossRef](#)] [[PubMed](#)]
35. Liang, L.; Yang, B.; Jiang, N.; Fu, W.; He, X.; Zhou, Y.; Ma, W.L.; Wang, X. Three-month Follow-up Study of Survivors of Coronavirus Disease 2019 after Discharge. *J. Korean Med. Sci.* **2020**, *35*, e418. [[CrossRef](#)] [[PubMed](#)]
36. Casali, M.; Lauri, C.; Altini, C.; Bertagna, F.; Cassarino, G.; Cistaro, A.; Erba, A.P.; Ferrari, C.; Mainolfi, C.G.; Palucci, A.; et al. State of the art of 18F-FDG PET/CT application in inflammation and infection: A guide for image acquisition and interpretation. *Clin. Transl. Imaging* **2021**, *9*, 299–339. [[CrossRef](#)] [[PubMed](#)]
37. Alonso Sanchez, J.; García Prieto, J.; Galiana Morón, A.; Pilkington-Woll, J.P. PET/CT of COVID-19 as an Organizing Pneumonia. *Clin. Nucl. Med.* **2020**, *45*, 642–643. [[CrossRef](#)] [[PubMed](#)]